STUDIA UBB CHEMIA, LXX, 4, 2025 (p. 75-95)
(RECOMMENDED CITATION)
DOI:10.24193/subbchem.2025.4.05

# STUDIES ON THE ADSORPTION OF CONGO RED ANIONIC DYE FROM SYNTHETIC AQUEOUS SOLUTIONS USING WASTE EGGSHELL BIOMASS

**Silvia BURCĂ[a] and Cerasella INDOLEAN[a,*]**

**ABSTRACT.** In this study, waste eggshells (WES) were investigated as an efficient biosorbent for the removal of Congo Red (CR) dye from aqueous solutions. The adsorption performance was quantified using UV–Vis spectroscopy at 498 nm. Fourier Transform Infrared (FTIR) spectroscopy confirmed the presence of hydroxyl, carbonyl, and methylene functional groups in WES, as well as structural modifications following CR adsorption.

Batch adsorption experiments were conducted to evaluate the effects of contact time, initial dye concentration, temperature, and pH on the adsorption capacity and efficiency. The highest CR removal efficiency (98.80 %) was achieved at pH 5.94, using a solid-to-liquid ratio of 5 g/100 mL and an initial CR concentration of 97.75 mg/L. The maximum adsorption capacity of WES was determined to be 9.12 mg CR/g WES. Optimized adsorption conditions were established using 4 g WES/100 mL at 295 K, pH 5.94, and an initial concentration of 97.97 mg CR/L under static conditions.

Thermodynamic analysis revealed the spontaneous and exothermic nature of the adsorption process, as indicated by a negative enthalpy change ($\Delta H = -40.708$ kJ mol$^{-1}$). These findings demonstrate the feasibility of employing waste eggshells as an effective and sustainable biosorbent for the removal of azo dyes from contaminated water.

***Keywords:*** *eggshell, Congo Red, adsorption, wastewater, thermodynamics*

[a] *Babeş-Bolyai University, Faculty of Chemstry and Chemical Engineering, 11 Arany Janos str., RO-400028, Cluj-Napoca, Romania.*
[*] *Corresponding author: liliana.indolean@ubbcluj.ro*

## INTRODUCTION

Safe drinking water and sanitation are human rights. Without access to these services, a life of stability and good health is virtually impossible [1].

According to the United Nations estimate, over 95 trillion gallons of wastewater are produced yearly. Only 20% of wastewater is currently treated, according to the reports released by the Global Commission on the Economics of Water (GCEW). It was predicted that by 2030, the fresh water demand will rise above availability by 40% [2].

The textile industry extensively uses dyes to colour its products, consuming substantial volumes of water in the process. Consequently, it generates large quantities of coloured wastewater. It is estimated that over 100,000 commercially available dyes are generated annually, with a total output exceeding 700,000 tonnes of dyestuff [3]. Approximately 5–10% of these dyes are lost in industrial effluents [4]. The direct discharge of such effluents into natural water bodies leads to significant environmental concerns, primarily due to their high organic load, toxicity, and persistent coloration. This contamination reduces light penetration and impairs photosynthesis, thereby negatively impacting aquatic ecosystems. Moreover, many dyes are known to be toxic, mutagenic, or even carcinogenic.

Particularly, an anionic diazo dye known as Congo red (CR) has been employed extensively for dyeing cotton, hemp, and silk fabrics and paper [5]. Congo red dye ($C_{32}H_{22}N_6Na_2O_6S_2$), having azo groups with aromatic ring and sulphonate groups, is a very harmful dye that is used in many industries. Due to its structural stability, CR is difficult to biodegrade. This dye is known to metabolize to benzidine, a known human carcinogen [6].

The eggshell is mainly the outer shield of the hard-shelled egg, and the weight of this shell is 11% of the overall weight of a single egg. The constituent materials of eggshells are $CaCO_3$, $MgCO_3$, $Ca_3(PO4)_2$, and various organic matters, while the percent distributions are 94%, 1%, 1%, and 4%, respectively [7, 8].

Various methods such as adsorption, coagulation, advanced oxidation, and membrane separation are used in the removal of dyes from wastewater [9]. Adsorption is one of the most effective processes of advanced wastewater treatment which industries employ to reduce hazardous inorganic/organic pollutants present in the effluent [10].

## RESULTS AND DISCUSSION

### *1. Optical Microscopy*

Optical microscopy images of the WES (waste eggshells) surfaces before and after Congo Red (CR) adsorption were obtained using a Motic BA310Pol microscope. As shown in Fig. 1, a noticeable difference in surface roughness is observed between the unmodified WES sample (Fig. 1a) and the CR-loaded WES (Fig. 1b). The WES sample presents an irregular, rough and porous surface, with high granularity, and several tubular holes distributed in the mass of the adsorbent. The initial WES surface exhibited a porous morphology (Fig. 1a)., while the WES-CR sample displayed a distinct change in both colour and surface morphology, indicating the successful fixation of CR dye within the WES pores (Fig. 1b).

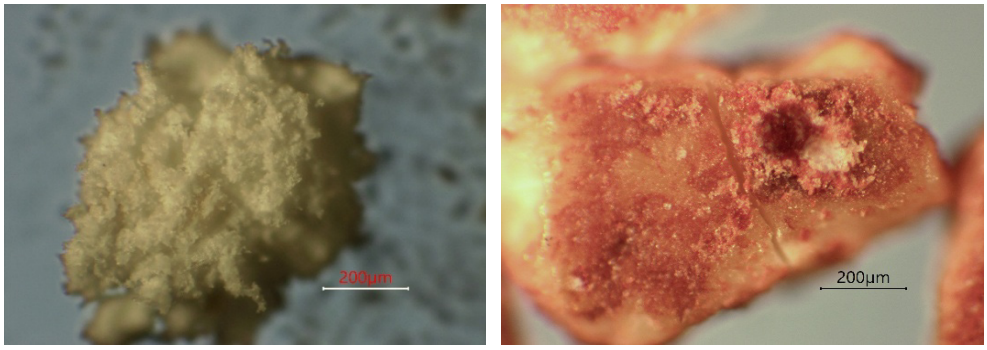


(a) (b)

**Figure 1.** Optical microscope images of the WES samples before (a) and after (b) CR adsorption.

### *2. The FTIR Analysis*

The FT-IR absorption spectra were recorded in reflection configuration with a Jasco 6000 spectrometer, at room temperature, in the range 400–4000 $cm^{-1}$; spectral resolution of 4 $cm^{-1}$; using the well-known KBr pellet technique.

From the spectral analysis, peaks at 407 $cm^{-1}$ and 405 $cm^{-1}$ are observed before and after the adsorption process, respectively. These fall within the fingerprint region. The band at 700 $cm^{-1}$ cans be assigned to vibrational modes associated to organic compounds with C-H, N-H, or C-O bonds [11]. After adsorption, these bands shift to 714 $cm^{-1}$, and remain ony one peak, indicating a structural change in the N-H, C-H or C-O groups due to interaction with the adsorbate. A band at 751 $cm^{-1}$ is present before adsorption and can be attributed to the out-of-plane deformation of the (=C–H) group. After adsorption, this band shifts slightly to 714 $cm^{-1}$, indicating a structural change in the (=C–H) group due to interaction with the adsorbate. Also, a rather important change is observed after CR adsorption on WES, in the sense that, the peaks at 595 and 640 $cm^{-1}$ disappear, and also, the peak at 751 $cm^{-1}$ is no longer founding the FTIR spectrum after CR uptake (Figure 1a, b). These important changes in the 500-800 $cm^{-1}$ area support the adsorption process of the CR dye onto biomass surface. Moreover, by consulting the data from the literature [12,13] it results that these transformations are specific of calcite zone. The bands at 714 $cm^{-1}$ and 877 $cm^{-1}$ (after adsorption) are also associated with in-plane and out-of-plane deformations of calcium carbonate [12]. Additionally, band at 1014 $cm^{-1}$ suggests stretching vibrations of the (C–O) functional group. A band at 1233 $cm^{-1}$ is detected before adsorption, which shifts to 1206 $cm^{-1}$ after the process, indicating deformation of the (C=S) group. The band at 1178 $cm^{-1}$ disappears after the adsorption of CR, suggesting changes in the C-O stretching vibrations of compounds such as alcohols, ethers, esters, etc. A distinct band at 1347 $cm^{-1}$ is attributed to the bending vibration of the C–H bond in alkane or aliphatic compounds from biocomposite (consisting of eggshell and its organic membrane), exhibits aromatic and aliphatic C–H stretching vibrations disappear also after CR uptake onto WES [7]. The band at 1653 $cm^{-1}$ in the absorption spectrum from Figure 1 (up), specific for the stretching vibrations of C=C in aromatic compounds, is shifted and modified in amplitude from 1658 $cm^{-1}$ (Figure 1 down). Additionally, the absorption band at 3498 $cm^{-1}$ corresponds to the O–H stretching vibration associated with hydroxyl groups from alcohols, phenols, etc., from the organic part of eggshells was shifted at 3504 $cm^{-1,}$ after adsorption. In addition, the bands at 2371, 2541, and 2930 $cm^{-1}$ that appear after the adsorption of CR are due to the characteristic functional groups of the CR dye structure [14].

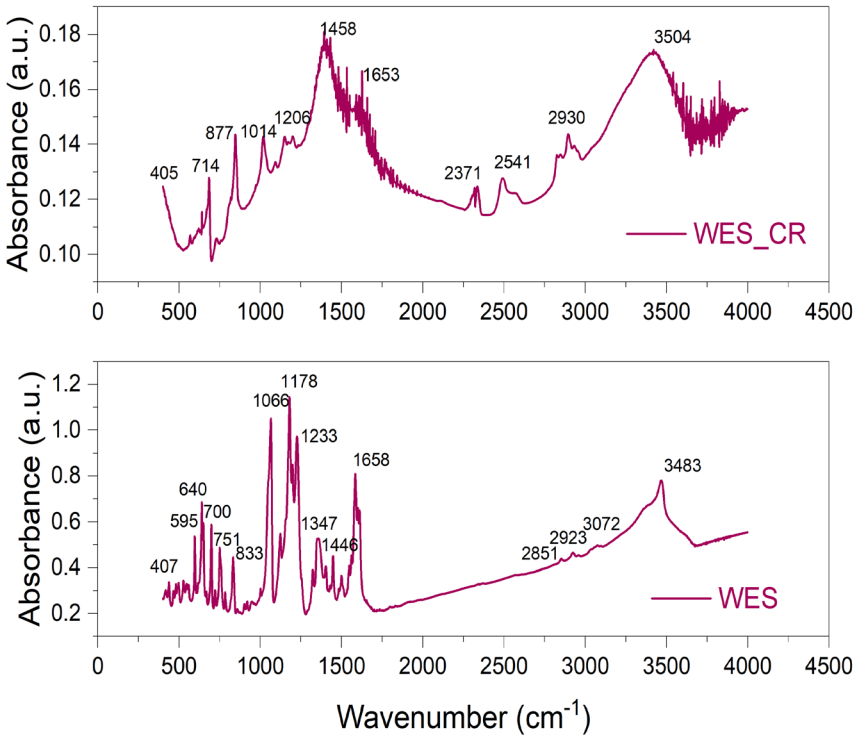


**Figure 2.** The FTIR spectra of the WES surfaces before (down) and after (up) CR adsorption.

## *3. Factors affecting efficiency of CR dye adsorption onto WES biomass*

### *3.1. Effect of biomass quantity*

The effect of biomass quantity on the adsorption of CR was studied using different masses of WES, ranging from 1 to 5 g/100mL CR solution.

Adsorption capacity determines the efficiency (E, %) and effectiveness of adsorption techniques for wastewater treatment.

Adsorption capacity refers to the quantity of adsorbate that a given mass of adsorbent can capture in specific conditions (Q, mg/g) [7].

Adsorption efficiency, expressed as percentage, was calculated with equation (1) [15.16]:

$$E = \frac{C_0 - C_e}{C_0} \times 100 \quad (1)$$

where $C_0$ and $C_e$ are the initial and equilibrium concentrations of CR, respectively (mg/L).

The amount of polutant (CR) adsorbed per gram of biomass (mg/g) was calculated using equation (2) [15,16]:

$$q_e = \frac{(C_0 - C_e) \cdot V}{m} \quad (2)$$

where V is solution volume (L) and m is WES quantity (g).

All presented values are the arithmetic mean of three series of data recorded from repetitions of the same experiment.

The effect of contact time on CR adsorption is presented in Fig. 3a. This evaluation is crucial, as it provides essential information regarding the time required to reach equilibrium. In all five cases (corresponding to 1–5 g of WES per 100 mL CR solution), equilibrium was achieved after 10 days under immobile phase conditions.

As shown in Fig. 3b, the maximum removal efficiency ranged from 98.61% (1 g WES) to 98.80% (5 g WES).

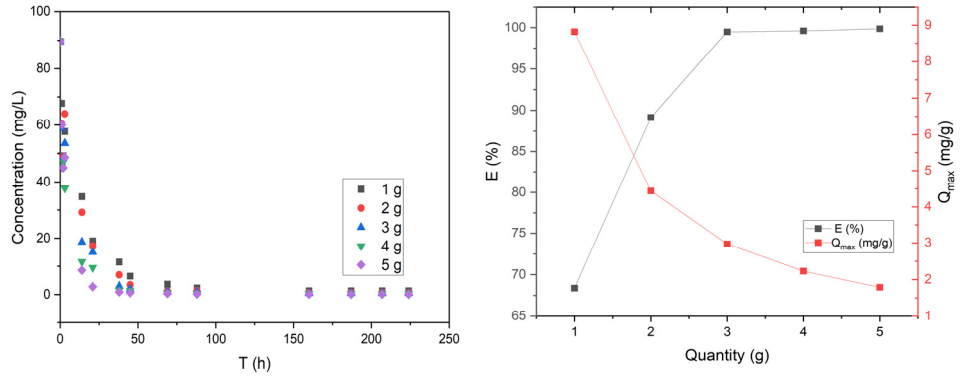


(a) (b)

**Figure 3.** (a) Influence of the WES biomass dosage over the time evolution of RC concentration, in batch conditions; (b) The effect of biomass quantity (1-5 g WES) on the adsorption of CR dye efficiency (E, %) and maximum adsorption capacity ($Q_{max}$, mg/g); 100 mL CR solution; $C_i$ = 97.75 mg CR/L; particle size, d < 0.2 mm, immobile phases regime, 10 days.

The highest efficiencies were obtained with 4 g (98.78%) and 5 g (98.80%) of WES. The use of 5 g/100 mL solution CR produced a dense suspension that was difficult to handle; therefore, a dose of 4 g WES was employed in subsequent experiments.

### *3.2. Effect of initial CR concentration*

In batch adsorption processes, the initial ion concentration of dyes in the solution plays an important role. Therefore, the amount of dye adsorbed is expected to be higher with a higher initial concentration of dye ions [14].

Also, the effect of initial CR concentration is closely related to the sites present on the adsorbent surface. In general, the percentage of dye removal decreases with increasing initial dye concentration, which leads to a saturation of adsorption sites on the adsorbent surface [15].

During the experiment, the adsorption of the anionic dye CR onto WES biomass was investigated at different initial dye concentrations ranging from 40.38 to 203.62 mg CR/L. The effect of contact time onto initial CR concentration is presented in Figure 4a. The results demonstrate that, regardless of the initial concentration of the dye solution, the residual concentration of CR in the solution approaches zero once equilibrium is reached (after 10 days). This observation supports the authors' claim that the biomass studied could constitute a very effective and valuable adsorbent material in future applications for water pollution remediation.

Figure 4b illustrates both the removal efficiency and the equilibrium adsorption capacity of CR as a function of the initial CR concentration.

In each test, 4 g of WES (particle size < 0.2 mm) was added to 100 mL of CR solution and left under immobile phases conditions at room temperature (295 ± 2K), without pH adjustment (initial pH of CR solution = 5.94). As shown in Figure 4b, the adsorption capacity of WES increased with increasing initial CR concentration, between 96.5 mg CR/g to 98.6 mg CG/g WES, while the efficiency increases in all 5 experiments from 67.70% for initial concentration of 40.38 mg CR/L to 99.91 % for 203.62 mg CR/L utilized.

### *3.3. Effect of particle size*

To evaluate the effect of particle size on the adsorption process, the WES material was ground and sieved into five different size fractions (< 0.2, 0.2-0.4, 0.4-1.0, 1.0-1.6 and >1.6 mm, Fig. 5a).

To establish the optimum adsorbent grain size, experiments were realized in the following conditions: 100 mL CR aqueous solution of Ci=97.75 mg/L was contacted with 1 g of WES, with grain sizes of d >1.6 mm; 1.6-1.0 mm; 1.0-0.4 mm; 0.4-0.2 mm or <0.2 mm. CR adsorption experiments were conducted in batch conditions, with immobile phases regime, at pH=5.94 and room temperature (T = 295K).

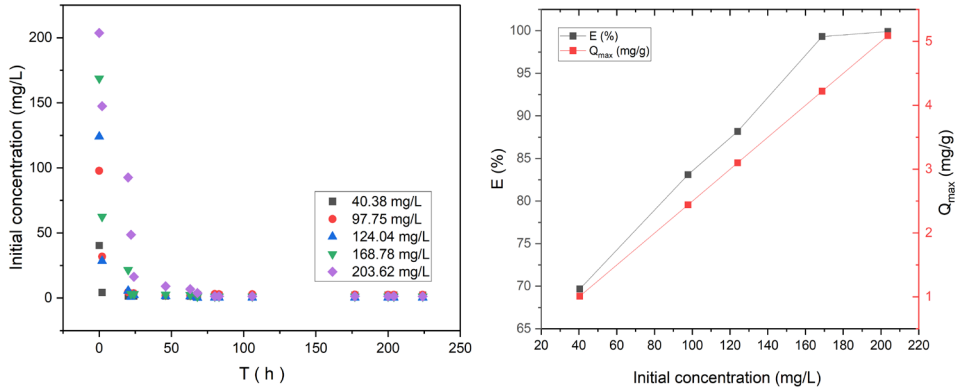


(a) (b)

**Figure 4.** (a) Effect of contact time on the initial concentration of CR dye using WES biomass**;** Ci =40.38–203.62 mg CR/L, 4 g WES, d < 0.2 mm, 295 K, pH =5.94, 10 days, immobile phases regime; (b) Influence of the initial CR dye concentration over the adsorption capacity and removal efficiency on WES biomass; Ci = 40.38–203.62 mg CR/L, 4 g WES, d < 0.2 mm, 295K, pH = 5.94, 10 days, immobile phases regime.

As can be seen (Figure 5a, b), the small particle sizes result in a larger specific surface area of WES, and consequently, increase the adsorption yield from 75.62 %, for d >1.6 mm to 96.62 % for d<0.2 mm WES grain sizes. When larger particles were ground into particles with smaller diameters, some tiny channels could be opened which might then become available for biosorption. This behaviour is in good agreement with other data from the literature [16].

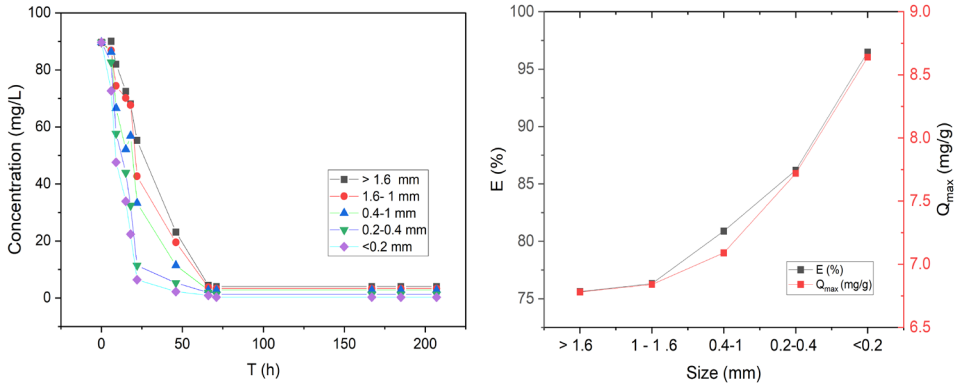


(a) (b)

**Figure 5.** (a) CR concentrations time evolution for different particle sizes of WES adsorbent (d >1.6 mm; 1.6-1.0 mm; 1.0-0.4 mm; 0.4-0.2 mm and <0.2 mm); (b) Representation of particle size effect of WES on CR adsorption efficiency (Ci = 97.75 mg CR/L, 1 g WES, 295 K, pH=5.94, 10 days, immobile phases regime).

The results obtained revealed that intraparticle diffusion within the pores of the WES adsorbent plays a significant role in governing the overall adsorption process. A substantial increase in adsorption capacity was observed with decreasing WES particle diameter, a behaviour consistent with trends previously reported in the literature [15, 17].

### *3.4. Effect of initial CR dye solution pH*

The pH is one of the most important controlling parameters in the biosorption process of dyes from wastewater [18].

The pH of aqueous solution can highly affect the WES surface charge. In acidic media, the surface of the adsorbent is protonated, while in a basic medium its surface deprotonates.

From the literature data result that adsorption was favourable in acidic media [19, 20].This may happen because of an electrostatic attraction between functional groups present in WES adsorbent and sulfonate ($SO_3^-$) group of CR [7].

The adsorption process was investigated by varying the pH of the aqueous solution within the range of 5.94–10.93. As presented in Figure 6, the highest adsorption efficiency for CR dye was obtained at pH 5.94 (99.7%), while in all cases the efficiency (E, %) remained above 98%. Upon

reaching adsorption equilibrium, the equilibrium concentration ($C_e$) corresponded to a final pH value of approximately 7 for all tested solutions (initial pH = 5.94, 6.68, 8.66, 9.46, and 10.93).

This result indicates that WES possesses an intrinsic buffering or neutralizing capacity, effectively stabilizing the pH of the dye solutions near neutrality regardless of the initial conditions.

In the future, this experimental finding could be extensively exploited, as WES appears to be a highly efficient adsorbent and a potential pH corrector.

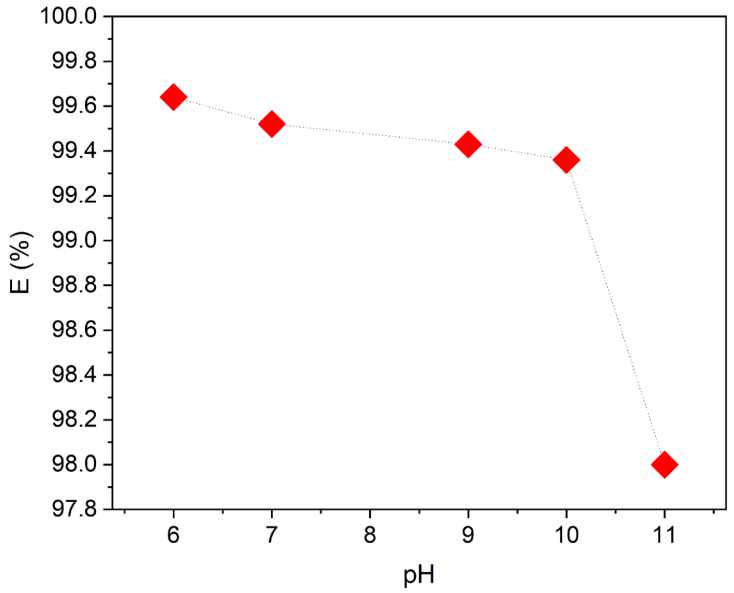


**Figure 6.** The effect of initial pH on percentage removal values for CR adsorption onto WES (Ci = 97.75 mg CR/L, 4 g WES/100 mL, d < 0.2 mm, 295 K, 10 days, immobile phases regime).

### *3.5. Thermodynamic aspects of CR adsorption onto WES biomass*

#### 3.5.1. Effect of temperature onto adsorption process

To describe the thermodynamic behaviour of the biosorption of CR onto WES biomass, standard thermodynamic parameters, including the changes in standard free energy (ΔG°), enthalpy (ΔH°) and entropy (ΔS°) were calculated using the following equations:

$$\Delta G^\circ = -RT \ln K_d \quad (3)$$

$$\Delta G^\circ = \Delta H^\circ - T\Delta S^\circ \quad (4)$$

where, R is the universal gas constant (8.314×10-3 kJ/K·mol), T is absolute temperature (K), and Kd is the distribution coefficient (L/g) calculated as $q_e/C_e$, where qe is biosorption capacity (mg/g) and $C_e$ is CR concentration in solution at equilibrium.

The enthalpy (ΔH°) and entropy (ΔS°) parameters were estimated from the equation Van't Hoff [15,19]:

$$\ln K_d = -\frac{\Delta H^\circ}{RT} + \frac{\Delta S^\circ}{R} \quad (5)$$

The effect of temperature on adsorption of 97.75 mg CR/L initial concentration of CR dye on 4 g/100 mL WES adsorbent dose was investigated. The experiments were completed at 295 K, 305 K, and 325 K (Fig. 7a). ΔH° and ΔS° values were obtained from the slope and the intercept of this plot, respectively. The standard free energy change (ΔG°), standard enthalpy change (ΔH°) and standard entropy change (ΔS°) were obtained using Equations (3) and (4) and their values associated with the adsorption of CR onto WES biomass are listed in Table 2.

From Fig. 7a, it can be noted that the effect of temperature has no very negative impact on adsorption capacity. Its values decrease, but not very much (between 2.430 mg/g, at 295 to 2.397 mg/g at 315K) as temperature increases from 295 to 325 K.

Further, the data obtained by plotting ln ($Q_e/C_e$) vs. 1/T were subject for thermodynamic study in order to establish the nature of adsorption process, Table 1 and Fig. 7b, shows the thermodynamic parameters of CR dye adsorption on WES.

**Table 1.** Thermodynamic parameters for CR adsorption onto WES at various temperatures (Ci = 97.75 mg CR/L, 40 g WES /L, d < 0.2 mm, pH=5.94).

| **$\Delta S^0$ kJ/K·mol** | **$\Delta H^0$ kJ/mol** | **$\Delta G^0$ kJ/mol** | | |
|---|---|---|---|---|
| | | **295 K** | **305 K** | **315 K** |
| -0.128 | -40.708 | -2.948 | -1.667 | -0.388 |

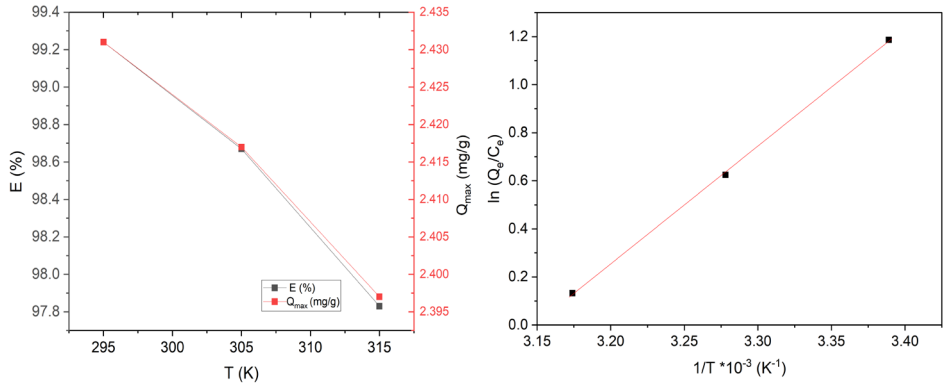


**Figure 7.** (a) The effect of temperature on removal efficiency for CR adsorption onto WES (b) Van't Hoff plot for the determination of thermodynamic parameters for the adsorption of CR onto WES as adsorbent (Ci = 97.75 mg CR/L, 4 g WES/100 mL, d < 0.2 mm, pH=5.94).

The values of ΔH, ΔS and ΔG are shown in Table 2. The negative values of ΔG that increased from -2.948 kJ/mol to -0.388 kJ/mol with an increase in temperature from 295 K to 315 K suggesting that adsorption can be dominated by weak physical interactions and that the physical adsorption predominate.

Also, the thermodynamic parameters indicate the feasibility of the process and the spontaneous nature of the adsorption.

The negative enthalpy change (ΔH = –40.708 kJ/mol) confirms the exothermic nature of the biosorption process, indicating that heat is released during the adsorption of the solute onto the WES adsorbent surface [21].

### 3.5.2. Mechanism of CR Dye Adsorption onto WES surface

Primarily, in aqueous solution, the Congo Red (CR) dye (CR–$SO_3Na$) undergoes dissolution and subsequent dissociation, yielding dye anions (CR–$SO_3^-$), as illustrated in Equation (7).

$$CR–SO_3Na \rightarrow CR–SO_3^- + Na^+ \quad (7)$$

The surface of WES is enriched with polar functional groups, primarily –$NH_2$ and –OH moieties (Figure 2). At low pH conditions (pH = 5.94), these groups undergo protonation, resulting in the formation of –$NH_3^+$ and –$OH_2^+$

species, respectively. Consequently, electrostatic interactions are likely established between these positively charged surface functionalities and the negatively charged dye anions, as illustrated in Equations (8) and (9).

$$–OH + H^+ \rightarrow –OH_2^+ + CR–SO_3^- \rightarrow CR–SO_3^-OH_2^+– \quad (8)$$

$$–NH_2 + H^+ \rightarrow –NH_3^+ + CR–SO_3^- \rightarrow CR–SO_3^-NH_3^+– \quad (9)$$

Therefore, the plausible adsorption mechanism can be attributed to a synergistic interplay of electrostatic attractions between the positively charged protonated functional groups of the adsorbent and the anionic species of the Congo Red (CR) dye, complemented by hydrogen bonding interactions and additional non-covalent forces such as π–π stacking and van der Waals interactions. [22, 23]

### 3.5.3. Effect of diffusion onto adsorption process

The intraparticle diffusion model proposed by Weber and Morris [24] was applied to elucidate the diffusion mechanisms governing the adsorption process.

The influence of intraparticle diffusion resistance on adsorption can be evaluated using the following relationship (Eq. 10), in which the intraparticle diffusion rate constant ($k_{ip}$, mg g$^{-1}$ min$^{-0.5}$) proposed by Weber and Morris was fitted to the experimental data:

$$Q_t = k_{ip}\, t^{1/2} + C \quad (10)$$

Weber–Morris intraparticle diffusion model, where $Q_t$(mg g$^{-1}$) is the amount of adsorbate at time $t$, $k_{ip}$(mg g$^{-1}$ min$^{-0.5}$) is the intraparticle diffusion rate constant, and $C$(mg g$^{-1}$) represents the boundary layer thickness or intercept (Table 2).

A larger $C$ value indicates a greater boundary layer effect, while a higher $k_{ip}$value reflects a faster diffusion rate within the adsorbent particles.

The diffusion mechanism was evaluated using the intraparticle diffusion model, which generally comprises three linear regions corresponding to film diffusion, pore diffusion, and adsorption equilibrium [25, 26]. The intraparticle diffusion plots for CR adsorption onto WES biomass (Figure 8a) display a multilinear trend, indicating that multiple diffusion processes govern the overall adsorption mechanism.

**Table 2.** Intra-particle diffusion rate coefficients and liquid film diffusion rate coefficients for CR uptake on WES biomass; $C_i$=40.38-124.04 mg CR/L, 4 g CR, d< 0.2 mm, 295 K, pH=5.94, immobile phases regime, 10 days.

| **Internal diffusion** | | | |
|---|---|---|---|
| Initial concentration (mg/L) | $k_{ip}$ (mg/g·h$^{0.5}$) | Intercept | $R^2$ |
| 124.04 | 0.332 | 1.472 | 0.904 |
| 97.75 | 0.229 | 1.315 | 0.998 |
| 40.38 | 0.033 | 0.828 | 0.985 |
| **External diffusion** | | | |
| Initial concentration (mg/L) | $K_{fd}$ (1/h) | Intercept | $R^2$ |
| 124.04 | 0.109 | 0.867 | 0.940 |
| 97.75 | 0.118 | 0.885 | 0.996 |
| 40.38 | 0.061 | 1.915 | 0.942 |

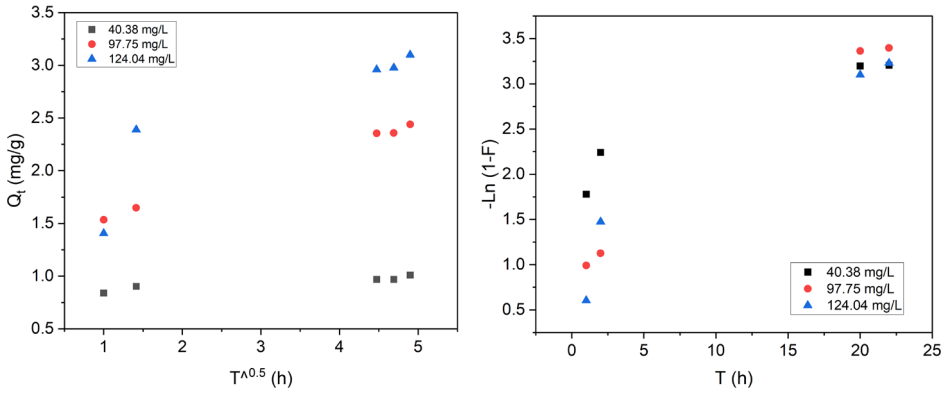


(a) (b)

**Figure 8.** Plots of the (a) intraparticle diffusion (Weber–Morris) and (b) liquid film diffusion (Boyd) model for CR adsorption using WES biomass; $C_i$ = 40.38, 97.75 and 124.04 mg CR/L, d<0.2mm, 295 K, pH 5.94, 10 days contact time, immobile phases regime**.**

Plots of $Q_t$versus $t^{1/2}$ were linear (with corresponding $R^2$values shown in Table 2), but the intercepts, C values, (0.828–1.472) did not pass through the origin for the initial CR concentrations of 124.04 and 97.75 mg/L, suggesting that intraparticle diffusion was not the sole rate-controlling step. At the lowest concentration (40.38 mg/L), a smaller intercept value indicates that intraparticle diffusion contributed more significantly to the adsorption

process. This behaviour implies that at low dye concentrations, reduced boundary layer resistance facilitates dye diffusion into the internal pores of the WES biomass, whereas at higher concentrations, both film and intraparticle diffusion jointly influence the adsorption rate.

If it is considered that external diffusion (through the liquid film on the surface of the adsorbent granule) can be the rate-determining step, the pore diffusion constant can be calculated using the equation derived by Boyd [27], the liquid film diffusion model (Table 2):

$$\ln(1-F) = -k_{fd} \cdot t \tag{11}$$

where, $F = q_t/q_e$ and $k_{fd}$ is the rate constant of diffusion through the liquid film, in L/min.

At higher initial concentrations (124.04 and 97.75 mg/L), the subunit intercept values (0.867 and 0.885, respectively; Table 2) further confirm that the adsorption process was primarily governed by external (film) diffusion. The higher concentration gradient likely enhanced mass transfer from the bulk solution to the biomass surface, favouring film diffusion over pore diffusion. These results are consistent with previous studies [7, 28, 29], indicating that external diffusion predominates at elevated solute concentrations.

Although the use of WES biomass represents a promising approach for the removal of Congo Red (CR) dye from wastewater, several inherent limitations remain, posing significant scientific and technological challenges for future research. These challenges include:

- *low adsorption capacity* – the primary constituent of WES, calcium carbonate ($CaCO_3$), possesses a relatively low specific surface area and a limited number of active functional sites, resulting in inferior adsorption performance compared to activated carbon, biochar, or surface-modified adsorbents.
- *limited structural stability and regeneration efficiency* — the desorption and subsequent reuse of WES-based adsorbents are often inefficient, which hinders their long-term applicability in cyclic adsorption–desorption operations.
- *management of spent adsorbent* — following dye adsorption, the disposal of dye-laden eggshell material must be carefully addressed, as improper handling, such as direct landfilling or incineration, may induce secondary environmental contamination.

In view of these limitations, future research should focus on enhancing the adsorption capacity of WES biomass, developing efficient strategies for the management and regeneration of spent adsorbent, and extending investigations to complex wastewater matrices containing multiple pollutants beyond Congo red dye.

## CONCLUSIONS

The whole eggshell matrix (WES), consisting of the eggshell and the eggshell membrane, represents a promising low-cost and eco-friendly adsorbent for dye removal from aqueous solutions. This study investigates the potential of WES as an adsorbent for Congo Red (CR) dye.

Results show that 1.0 g of eggshell material was sufficient to remove more than 90% of the pollutants analyzed. The WES effectively adsorbed CR at low concentrations, although the percentage removal decreased with increasing dye concentration. Adsorption equilibrium was reached after 10 days, under static conditions (in immobile phases regime). The maximum biosorption efficiency (99.93%) was obtained at pH 5.94 and 295 K, using a 97.75 mg $L^{-1}$ CR solution and 4 g of WES with a 10-day contact time.

The adsorption process was found to be pH-dependent, with optimum performance at pH 5.94. The effect of pH on sorption capacity was mainly attributed to ionic interactions between the surface of the WES and the CR molecules. Due to the porous structure of the eggshell—composed predominantly of calcium carbonate and offering a high surface area for dye interaction—WES exhibited remarkable adsorption behavior across a range of initial pH values. Interestingly, regardless of the initial pH of the synthetic wastewater, the final pH after adsorption consistently reached neutrality (pH=7).

Temperature (295, 305, and 315 K) had a noticeable but limited influence on dye adsorption. The observed temperature dependence was attributed to the increased mobility of CR ions, which may desorb from the solid phase back into the solution at higher temperatures.

Overall, the findings demonstrate that WES is an efficient, sustainable, and low-cost biosorbent for the decolorization of synthetic wastewater containing Congo Red dye.

## EXPERIMENTAL SECTION

### *Biosorbent*

The biomass used as adsorbent material for the removal of CR dye from wastewater was chicken eggshells, a residue that can be easily procured and found in large quantities. The adsorbent material (WES) was employed without any preliminary chemical treatment. It was thoroughly washed with distilled water, oven-dried at 105℃.

### *Sieving and Particle Size Fractionation*

The dried sample was subjected to mechanical sieving to separate it into defined particle size fractions. A stainless steel sieve set (Retsch AS 200) was used, comprising sieves with mesh openings ranging from > **1**.6 mm to <0.2 mm (corresponding to sieve sizes: >1.6 mm, 1.0-1.6 mm, 0.4-1.0 mm, 0.2-0.4 mm, 125 µm, and <0.2 mm).

Approximately 100 g of the dried material was placed on the uppermost sieve, and the stack was secured and mounted on the mechanical shaker. Sieving was performed for 10 minutes at an amplitude of 1.5 mm (vibration intensity setting 70%) to ensure efficient separation without particle degradation. After sieving, each fraction retained on the sieves was carefully collected, weighed, and stored in airtight containers for further analysis.

(a) (b)

**Figure 9.** (a) The general macroscopic aspect of eggshells, before their physical processing; (b) Adsorption experiments of CR removal by WES, in a regime with immobile phases.

The sieved biosorbent was then stored in an airtight box before its utilization. No further chemical treatments were considered at this stage. Optical microscope images of biosorbent were obtained with an apparatus on samples.

### *Chemicals*

Congo Red (CR, Direct Red 28, C.I. 22120, azo dye, $C_{32}H_{22}N_6Na_2O_6S_2$, molecular weight 696.7, selected as anionic dye) was purchased from Penta (Czech Republic) and used without further purification. The stock solution, 1000 mg/L of Congo Red was prepared by dissolving the solid in distilled water. The required concentrations were obtained by diluting the stock solution to the desired concentrations, in 40–200 mg/L range. CR concentration was determined using a double beam UV-visible spectrophotometer (GBC Cintra 202) at λ = 498 nm. HCl (0.1 M) and NaOH (0.1 M) volumetric solutions were used to adjust the solution pH. All chemicals used were of analytical grade.

### *Biosorption Experiments*

The biosorption experiments were carried out under batch conditions in a static regime, by contacting a defined mass of adsorbent (1–5 g) with 100 mL of Congo Red (CR) dye aqueous solution at concentrations ranging from 40 to 204 mg $L^{-1}$. Adsorption was allowed to proceed until equilibrium was reached, as determined from preliminary experiments. The residual dye concentration in the solution was determined at predefined time intervals following preliminary centrifugation (5 min at 6000 rpm) and appropriate dilution.

The solid fraction of WES was separated by centrifugation using a Hettich EBA 200 centrifuge equipped with an angled rotor, operated at a relative centrifugal force (RCF) of approximately 3461×g. Solid–liquid separation of the eggshell-derived adsorbent from the supernatant was routinely conducted using this procedure. The absorbance of the supernatant was measured at the maximum wavelength ($\lambda_{max}$) of CR, and dye concentrations were calculated from the corresponding calibration curve.

To evaluate the effect of temperature on the adsorption process, experiments were conducted at 295, 305, and 315 K using 100 mL of CR solution (97.75 mg $L^{-1}$) and 4 g of WES.

Fourier transform infrared (FTIR) spectra of the adsorbent before and after adsorption were recorded in triplicate using a Varian FT-IR 670 spectrometer over the range 4000–400 $cm^{-1}$. Each sample was finely ground, mixed with KBr at a mass ratio of 1:50 (sample:KBr), and pressed into pellets for analysis.

### *Stability of CR dye solutions*

To determine the wavelength corresponding to the maximum absorbance ($\lambda_{max}$) and its variation with pH, a 5 mg $L^{-1}$ solution of CR was prepared. The pH of the solution was adjusted over the range of 5.94 to 10.93 using 0.1 M HCl or 0.1 M NaOH. Visible absorption spectra were then recorded at room temperature using a double-beam UV–Vis spectrophotometer (GBC Cintra 202). The maximum absorbance was observed at a wavelength of 498 nm.

Decolorization was quantified by correlating the absorbance at this wavelength. The CR dye adsorbed by the WES biomass was calculated from the difference between initial concentration and the final concentration in the supernatant and was calculated using the equations (1) and (2).

## ACKNOWLEDGMENTS

The authors express their gratitude to their colleague, lecturer Cosmin Coteţ, PhD, for performing the optical microscopy analyses.

Also, the authors thank Mrs. Miuţa Filip for recording the FTIR spectra.

## REFERENCES

1. UN World Water Development Report 2024 | UN-Water
2. J. Ambigadevi and P. Senthil Kumar, *Int. J. Chem. Eng.,* **2025**, *1*, 1-19 https://doi.org/10.1155/ijce/5541488.
3. Kusumlata, B. Ambade, A. Kumar, S. Gautam, *Limnol. Rev.,* **2024**, *24*(2), 126-149; https://doi.org/10.3390/limnolrev24020007.
4. K. Litefti, M.S. Freire, M. Stitou, J. G. Álvares, *Nature Sci. Rep.*, **2019**, *9*, 16530; https://doi.org/10.1038/s41598-019-53046-z.
5. H. Bai, Y. Feng, C. Zhu, P. Guo, J. Wang, Y. Zhou, L. Zhang, S. Li, J. Chen, *J. Taiwan Inst. Chem. Eng*, **2024**, *164*, 105689 - 105695. https://doi.org/10.1016/j.jtice.2024.105689.
6. V. S. Mane and P.V.V. Babu, *J. Taiwan Inst. Chem. Eng.*, **2013,** *44(1)*, 81-88. https://doi.org/10.1016/j.jtice.2012.09.013

7. P. E. Emumejaye, S. C. Ikpeseni, M. Ekpu, S. O.-O. Sada, P. O. Ohwofadjeke, J. Sci. Technol. Res., **2023**, *5(4)*, 128-137.
8. S. Parvin, Al-M., F. Rubbi, Md. A. Ruman, Md. M. Rahman, B. K. Biswas**,** *Aceh. Int. J. Sci. Technol.,* **2020**, *9(2)* 63-74*,* https://doi: 10.13170/aijst.9.2.16767
9. M.T. Yagub, T. K. Sen, S. Afroze, H.M. Ang, *Adv. Col Interface Sci*, **2014**, *209*, 172-184, https://doi.org/10.1016/j.cis.2014.04.002.
10. S. Satyam, S. Patra, *Helyion*, 2024, *10(9)*, e29573 - 29597. https://doi.org/10.1016/j.heliyon.2024.e29573.
11. P.E. Emumejaye, S.C. Ikpeseni, M. Ekpu, S.O.O. Sada, P. Ohwofadjeke, *J. Sci. Technol. Res.,* **2023**, *5(4)*, 128-137.
12. R. de Oliveira Zonato, B. R. Estevam, I. D. Perez, V. A. dos Santos Ribeiro, R.F. Boina, *Clean Chem. Eng.,* **2022**, *2*, 100023-100032. https://doi.org/10.1016/j.clce.2022.100023.
13. A.Soltani, M. Faramarzi, S.A. Mousavi Parsa *Water Quality Res. J.*, **2021**, *56 (4)*,181-193. https://doi.org/10.2166/ wqrj.2021.023.
14. R.A Nassif., *J. Multidiscipl. Eng. Sci. Technol.*, **2019**, *6(9)*, 10611-10613.
15. M.K. Dahri, M.R.R. Kooh, L.B.L. Lim, *J. Environ. Chem. Eng*., 2014, *2(3)*, 1434-1444 https://doi.:10.1016/j.jece.2014.07.008.
16. M. Harja, G. Buema, D. Bucur, *Nature. Sci. Reports,* **2022**, *12*, 6087-6105. https://doi.org/10.1038/s41598-022-10093-3
17. K. M. Ravi, G. M., Wondalem, P.S. Satya, J.J. Lakshmi, A.S. Ashager, P. King, M. Vijay, G. Baburao, *Chem. Methodol*., **2023**, *7*, 605-612. https://doi.org/10.22034/CHEMM.2023.395359.1676.
18. S. Burcă, A.Măicăneanu, C. Indolean, *Rev. Roum. Chim.*, **2014**, *59(10),* 817-824.
19. M.A. Abdel-Khalek, M.K. Abdel Rahman, A.A. Francis, *J. Environ. Chem. Eng.*, **2017**, *5(1)*, 319-327. https://doi.org/10.1016/j.jece.2016.11.043
20. N. K. Kınaytürk, B. Tunalı, D.T. Altug, *R. Soc. Open Sci*., **2021**, *8*, 210100-210114. https://doi.org/10.1098/rsos.210100
21. J. R. Njimou, A. Măicăneanu, C. Indolean, C.P. Nanseu-Njiki, E. Ngameni, *Environ. Technol.*, **2016**, *37(11)*, 1369–1381. http://dx.doi.org/10.1080/09593330.2015.1116609
22. N. F. Al-Harby, E. F. Albahly, N. A. Mohamed, *Polymers*, **2021**, *13(24)*, 4446-4478. https://doi.org/10.3390/polym13244446
23. R. Kumar, S.A. Ansari, M.A. Barakat, A. Aljaafari, M.H. Cho, *New J. Chem*., **2018**, *42*, 18802–18809.
24. W.J. Weber, J.C. Morris, J.C., 1963) *J. Sanitary Eng. Div., Am. Soc. Civil Eng*., **1963**, *89*, 31-60.
25. Meghana, C., Juhi, B., Rampal, N., Vairavela, P., *Desalination Water Treat*., **2020**, *207*, 373–397, http://doi: 10.5004/dwt.2020.26389
26. K.Wu, X.Pan, J. Zhang, Xi. Zhang, A. Salahzene, Y. Tian, **2020**, *ACS Omega, 5(38)*, 24601-24612. https://doi.org/10.1021/acsomega.0c03114.
27. J. Wang , X. Guo, *J. Hazard. Mater.,* **2020**, *390*, 122156-12274. https://doi.org/10.1016/j.jhazmat.2020.122156

28. P. S Kumar, S.J. Varjani, S. Suganya, *Bioresour. Technol.*, **2017**, *250*, 716−722. https://doi.org/10.1016/j.biortech.2017.11.097
29. G.O. Ogunlusi, O.D. Amos, O.F. Olatunji, *J Iran. Chem. Soc.,* **2023**, *20*, 817–830. https://doi.org/10.1007/s13738-022-02721-6.